BIO-MIMETIC SUBWAVELENGTH SURFACES FOR NEAR-ZERO REFLECTION SUNRISE TO SUNSET

S. A. Boden and D.M. Bagnall
Nanoscale Systems Integration, Electronics and Computer Science
University of Southampton, Highfield, Southampton, SO17 1BJ, United Kingdom

ABSTRACT

We present a study of antireflective schemes and their operation over a full day. We compare simulation results for single and double layer antireflective coatings with bio-mimetic moth-eye structures, taking into account the full range of wavelengths and incident angles experienced by fixed solar cells from sunrise to sunset. We show that solar cells incorporating antireflective moth-eye arrays could produce up to 12% more energy than those employing single layer antireflective coatings.

INTRODUCTION

Thin film antireflection coatings (ARCs) are commonly used to achieve antireflection in solar cells [1]. Materials and thicknesses for thin film ARCs are chosen to cause destructive interference between light of particular wavelengths reflected from the different interfaces created by the presence of the thin films. Destructive interference leads to a minimization of reflected light at the design wavelength(s) [2]. In this way, very low reflectances are achieved for relatively narrow ranges of wavelength and incident angle, which suggests that this is not an ideal method of minimizing reflection for all conditions. There are also difficulties with the availability of materials with suitable optical properties and problems with delamination of layers.

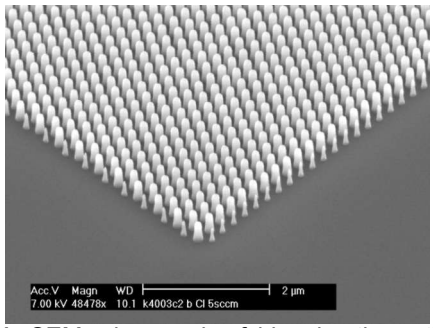

Fig. 1. SEM micrograph of bio-mimetic moth-eye array in silicon.

Inspired by nature, researchers are developing an alternative to thin film ARCs: Subwavelength-structured arrays. The surfaces of cornea of some night-flying moths are covered with arrays of subwavelength structures (see Fig. 1) which confer an antireflective effect [3, 4]. Incident light cannot resolve the individual features on the surface and so the patterns exhibit an effective refractive index dependent on the ratio of the corneal material to air. The shape of the features causes this ratio to gradually increase from air into the cornea, leading to a gradual increase in effective refractive index. This eliminates the discontinuity in refractive index at the interface and so minimizes reflection. Studies show that these surfaces exhibit low reflectivities over broad ranges of wavelength and angle of incidence [5, 6] and so could be more effective than thin film ARCs for reducing reflection over a day.

Traditionally, device manufacturers have concentrated on efficiency values for standardized irradiances (i.e. AM 1.5) at normal incidence, and as a consequence, most antireflection schemes have been optimized for conditions that prevail for fixed systems only for a small part of a day. For a more accurate assessment of the performance of antireflective schemes for PV applications it is important to account for the full range of incident angles and solar spectral intensities experienced by a solar cell from sunrise to sunset. In this paper we present simulation results that allow us to compare single and double layer ARCs with two implementations of the moth-eye structure.

SIMULATION METHOD

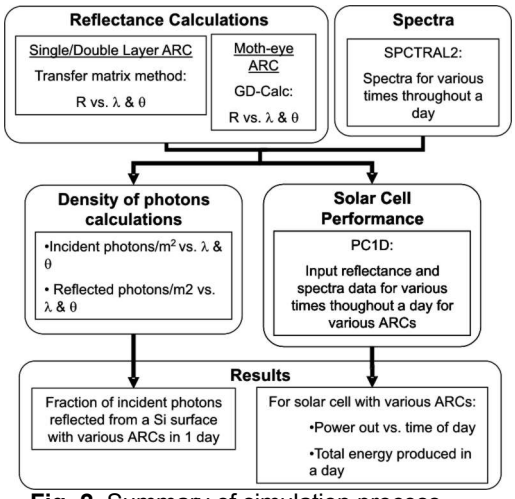

Fig. 2. Summary of simulation process.

The simulation process is summarized in Fig. 2. Reflectance as a function of wavelength (in the range from 300 nm to 1240 nm) and angle of incidence (from 0-90º) is calculated using a transfer matrix method for thin film ARCs [2] and using GD-Calc, a commercially available diffraction grating program [7], for moth-eye ARCs.

The transfer matrix method involves matching the tangential components of electric and magnetic fields across adjacent interfaces in the single, double or multi layer stack for two polarization states: the electric field perpendicular to the plane of incidence (TE) and the electric field parallel to the plane of incidence (TM). This forms a characteristic matrix M_j for relating the fields at each adjacent interface.

$$M_j = \begin{bmatrix} \cos k_0 h_j & \left(i \sin k_0 h_j\right)/\mathrm{Y}_j \\ \mathrm{Y}_j i \sin k_0 h_j & \cos k_0 h_j \end{bmatrix} \quad (1)$$

$$\begin{bmatrix} E_I \\ H_I \end{bmatrix} = M_I \begin{bmatrix} E_{j+1} \\ H_{j+1} \end{bmatrix} \quad (2)$$

where

$$k_0 = \frac{2\pi}{\lambda_0} \quad (3)$$

$$h_j = n_j d_j \cos\theta_j \quad (4)$$

$$\mathrm{Y}_j = \sqrt{\frac{\varepsilon_0}{\mu_0}} n_1 \cos\theta_j \quad \text{(for TE waves)} \quad (5)$$

$$\mathrm{Y}_j = \sqrt{\frac{\varepsilon_0}{\mu_0}} n_1 / \cos\theta_j \quad \text{(for TM waves)} \quad (6)$$

and n_j and d_j are the refractive index and thickness of layer j respectively and θ_j is the angle of incidence for layer j.

The product of the characteristic matrices is a characteristic matrix for the whole ARC system and from this, reflectance as a function of wavelength and incident angle is calculated. Sunlight can be assumed to be randomly polarized so the average reflectance of the two polarizations calculated was used. Full details of the method can be found in ref. [2].

GD-Calc uses a generalization of the rigorous coupled-wave method detailed in [8]. The moth-eye array is defined by strata in a staircase-like approximation, as shown in Fig. 3. GD-Calc calculates the diffraction efficiencies of the transmitted and reflected diffracted orders. By summing the efficiencies of the reflected orders, we could obtain the total reflection as a function of angle of incidence and wavelength.

A solar spectrum calculator, SPCTRAL2 [9], is then used to determine the number of photons per m^2 incident on a cell as a function of wavelength and angle of incidence over a day.

Solar spectral irradiance data for both direct and diffuse light were obtained and irradiance as a function of wavelength was calculated for every 5 minutes throughout half a day, which corresponds to a range of angles of incidence (for the direct light) from 0 to 90 degrees.

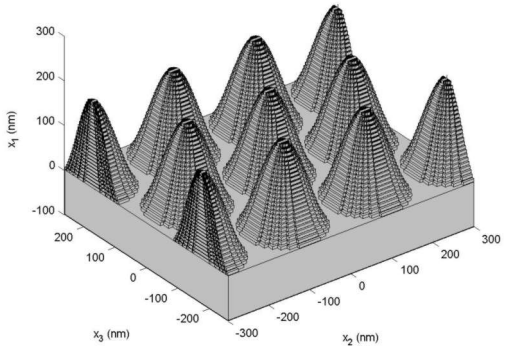

Fig. 3. Grating defined in GD-Calc as an approximation of subwavelength texturing for antireflection.

We assume the day is symmetrical about noon in terms of angle of incidence so we only need to consider data for a half-day. The raw direct-light data were multiplied by the cosine of angle of incidence to take into account the increase in projected area as the angle of incidence is increased. The data were integrated to obtain irradiance in units of W/m^2 and the diffuse-light irradiance was averaged out over the half-day as this contribution is spread out over the range of incident angles. The direct and diffuse spectra were then added together to obtain the total irradiance over half a day as a function of time (or equivalently, angle of incidence) and wavelength. This was converted into the total density of photons, in units of photons/m^2 (see Fig. 4).

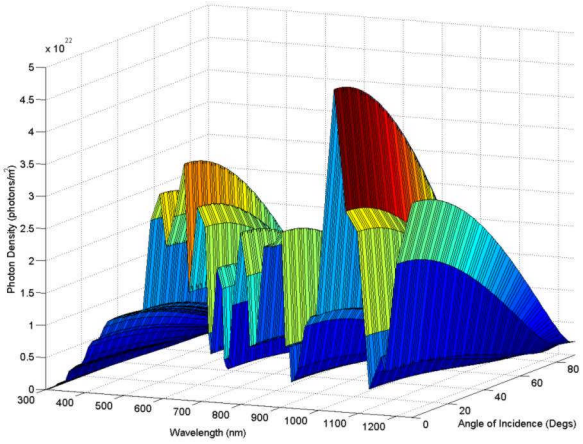

Fig. 4. Total density of photons as a function of wavelength and angle of incidence, calculated using values from SPCTRAL2.

Multiplying the spectral data with the reflectance data and then summing gives the total number of photons reflected from the surface in half a day.

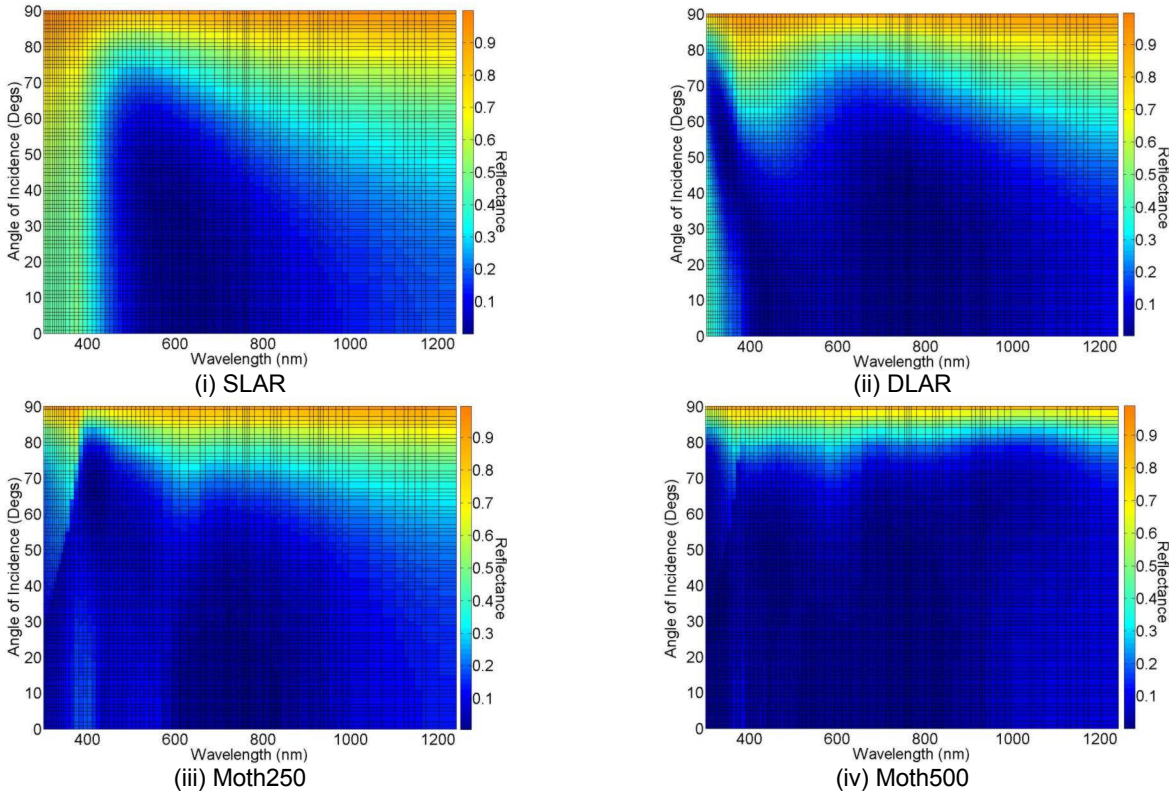

Fig. 5. Reflection vs wavelength and angle of incidence for various ARCs.

Reflectance and spectral data were also combined in the solar cell simulator PC1D [10] to simulate the performance of a solar cell coated with various thin film and moth-eye ARCs. Reflectance and spectra data for the different coatings and time of day/angles of incidence were input and the maximum power produced by a cell as a function of time of day was plotted for each ARC. Integrating these curves gives the total energy produced by the cell of a day.

Results for two thin film ARCs and two moth-eye arrays are presented. Details of these are given in Table 1.

Table 1. Descriptions of ARCs modeled (n = refractive index, d = layer thickness).

SLAR	CeO, n = 1.953, d = 78 nm (optimized in [1])
DLAR	MgF_2, ZnS, n_1 = 1.38, n_2 = 2.3, d_1 = 107 nm, d_2 = 56 nm (optimized in [1])
Moth250	Pillar height = 250 nm
Moth500	Pillar height = 500 nm

The variation in refractive index of silicon with wavelength is accounted for using values from ref. [11] but the refractive indices of the thin-film coatings were assumed to be constant because they vary little over the wavelength range of interest. We did not take into account the imaginary components of refractive index. This will introduce errors in the results for the short wavelengths but these will have little effect because the photon flux is low in this wavelength range.

RESULTS AND DISCUSSION

Reflection as a function of wavelength and angle of incidence for various thin-film and moth-eye based ARCs are presented in Fig. 5. The figures show that the Moth250 has similar antireflective properties to DLAR. An improvement is observed in Moth500, which exhibits excellent antireflectivity over broader wavelength and angle of incident ranges than the other ARCs. This is confirmed by the results in Table 2. The SLAR is the worst performer, as expected, with 18% of the total number of photons incident on the surface over a day being reflected. Using either DLAR or Moth250 reduces this to approximately 11-12%. Increasing the pillar depth to 500 nm, as in Moth500, results in a much lower percentage (5.4%) of incident photons reflected.

Table 2. Numerical results from simulations of a cell coated with various ARCs.

	No. of photons/m^2 reflected over a day (x10^{25})	**% of incident photons reflected over a day (%)**	**Energy produced by 1 cm cell over a day (J)**
SLAR	1.56	18.2	227.2
DLAR	0.96	11.2	237.5
Moth250	1	11.7	270.2
Moth500	0.46	5.4	281.8

Results from PC1D simulations are presented in Fig. 6. At sunrise at 6:00 a.m., the power produced is at a minimum because direct light is incident at an angle close to 90º, so reflection is high, and the intensity is low due to the amount of atmosphere the light has to pass through before reaching the cell. Throughout the morning, the angle of incidence reduces, corresponding to an increase in power, reaching a maximum at noon when direct light is at normal incidence, reflectance is at a minimum and intensity is maximum. The behavior is repeated in reverse in the afternoon leading to zero power at sunset. In agreement with previous results, the Moth500 curve is higher than the others throughout the day. The Moth250 and DLAR curves are approximately coincidental and the cell with the SLAR produces the lowest power throughout the day. Integrating the curves will give the total energy produced by the cell throughout the day. Results from these calculations are shown in
Table 2.

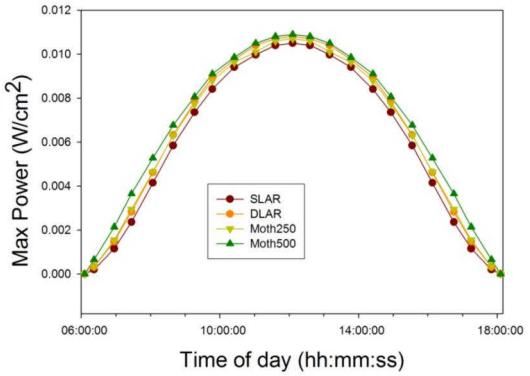

Fig. 6. Power produced by a solar cell with various ARCs from sunrise to sunset (spring equinox, Lat = 0°, Long = 0°).

The absolute values are not important because the cell we used in the model was not a high performance cell. Instead, a comparison of the values for cells coated with the different ARCs will provide a valuable assessment of their relative performances. Again, DLAR and Moth250 show a similar gain of ~5-6%. Replacing SLAR with Moth500 leads to 12% more energy from a solar cell from sunrise to sunset.

Increasing the height of the pillars in the moth-eye arrays improves the antireflective properties because the effective refractive index is made to vary over a longer distance, resulting in a more gradual change. Indeed, increasing the pillar height further would result in a lower reflectance, though fabrication would become increasingly difficult.

Our calculations have not included a possible increase in surface recombination using a moth-eye array to replace a thin film ARC. This effect could be significant and we aim to take this into account in future modeling.

CONCLUSIONS

Our simulations show that moth-eye arrays with 250 nm pillars exhibit antireflection performance similar to an optimized double layer ARC. Increasing the height of the pillars to 500 nm improves the antireflectivity further with the percentage of photons reflected over a day dropping to 25% of the value for an optimized single layer ARC. This results in an extra 12% of energy being produced by a cell with Moth500 compared to a cell with the SLAR coating. These simulations suggest that moth-eye arrays are promising alternatives to thin film ARCs and further investigations into the effect of varying the pillar profile, pillar height and the arrangement of pillars in the array are underway.

REFERENCES

[1] J. Zhao and M. A. Green, "Optimized Antireflection Coatings for High-Efficiency Silicon Solar-Cells," *Ieee Transactions on Electron Devices*, vol. 38, pp. 1925-1934, 1991.

[2] E. Hecht, *Optics*, 4th ed. San Francisco: Addison Wesley, 2002.

[3] P. Vukusic and J. R. Sambles, "Photonic structures in biology," *Nature*, vol. 424, pp. 852-855, 2003.

[4] C. G. Bernhard, "Structural and functional adaption in a visual system," *Endeavour*, vol. 26, pp. 79-84, 1967.

[5] P. B. Clapham and M. C. Hutley, "Reduction of Lens Reflexion by the "Moth Eye" Principle," *Nature*, vol. 244, pp. 281-282, 1973.

[6] S. J. Wilson and M. C. Hutley, "The Optical-Properties of Moth Eye Antireflection Surfaces," *Optica Acta*, vol. 29, pp. 993-1009, 1982.

[7] K. C. Johnson, "GD-Calc," 2005, pp. see http://www.software.kjinnovation.com/.

[8] M. Nevière and E. Popov, *Light Propagation in Peirodic Media*. New York: Marcel Dekker, Inc., 2003.

[9] R. E. Bird and C. J. Riordan, "SPCTRAL2- Bird Simple Spectral Model," 2004, pp. see http://rredc.nrel.gov/solar/models/spectral/.

[10] D. A. Clugston and P. A. Basore, "PC1D Version 5: 32-Bit Solar Cell Modeling on Personal Computers," presented at 26th IEEE Photovoltiac Specialists Conference, Anaheim, 1997.

[11] M. A. Green, *High Efficiency Silicon Solar Cells*. Aedermannsdorf: Trans Tech Publications Ltd., 1987.